EUR 3564 e

EUROPEAN ATOMIC ENERGY COMMUNITY - EURATOM

A METALLOGRAPHIC AND X-RAY INVESTIGATION OF PLUTONIUM OXIDES AT ROOM TEMPERATURE

by

C. SARI, U. BENEDICT and H. BLANK

1967

Joint Nuclear Research Center
Karlsruhe Establishment - Germany

Institute of Transuranium Elements

LEGAL NOTICE

This report is on sale at the addresses listed on cover page 4

at the price of FF 7.—	FB 70.—	DM 5.60	Lit. 870	Fl. 5.10

When ordering, please quote the EUR number and the title, which are indicated on the cover of each report.

Printed by Vanmelle s.a.
Brussels, August 1967

EUR 3564 e

EUROPEAN ATOMIC ENERGY COMMUNITY - EURATOM

A METALLOGRAPHIC AND X-RAY INVESTIGATION OF PLUTONIUM OXIDES AT ROOM TEMPERATURE

by

C. SARI, U. BENEDICT and H. BLANK

EUR 3564 e

A METALLOGRAPHIC AND X-RAY INVESTIGATION OF PLUTONIUM OXIDES AT ROOM TEMPERATURE by C. SARI, U. BENEDICT and H. BLANK

European Atomic Energy Community — EURATOM
Joint Nuclear Research Center — Karlsruhe Establishment (Germany)
Institute of Transuranium Elements
Brussels, August 1967 — 56 Pages — 38 Figures — FB 70

Plutonium oxides in the range $1.61 \leqq O/Pu \leqq 2.00$ have been investigated at room temperature both by metallography and by x-ray analysis, mainly on samples quenched from about 1500° C to 5° C. Specimens with compositions $1.627 < O/Pu \leqq 1.69$ are single phase α-type at 650° C and this phase can be quenched to room temperature to a high degree. Specimens with $1.69 < O/Pu \leqq 1.995$ invariably transform to a two-phase structure $\alpha + \gamma$ ($\gamma = PuO_{2-x}$) on quenching through the 650° phase boundary known from previous published phase diagrams. These phase diagrams have to be modified on the basis of the present results in two respects :

Joint Nuclear Research Center
Karlsruhe Establishment - Germany

Institute of Transuranium Elements

SUMMARY

Plutonium oxides in the range $1.61 \leq O/Pu \leq 2.00$ have been investigated at room temperature both by metallography and by x-ray analysis, mainly on samples quenched from about 1500° C to 5° C. Specimens with compositions $1.627 < O/Pu \leq 1.69$ are single phase α-type at 650° C and this phase can be quenched to room temperature to a high degree. Specimens with $1.69 < O/Pu \leq 1.995$ invariably transform to a two-phase structure $\alpha + \gamma$ ($\gamma = PuO_{2-x}$) on quenching through the 650° phase boundary known from previous published phase diagrams. These phase diagrams have to be modified on the basis of the present results in two respects :

I) α-Pu_2O_3 which has been taken earlier as a compound with O/Pu = 1.61 exists as an extended phase in the range $1.62 < O/Pu \leq 1.69$ at $T > 650°$ C. This range becomes narrower with decreasing temperature and terminates in a point near $O/Pu \approx 1.62 \div 1.63$ at about 350° C.

II) The oxygen deficient fluorite phase PuO_{2-x} at 350° C in equilibrium with the α-phase has a composition close to PuO_2, that is about $PuO_{1.995}$ instead of $PuO_{1.98}$ as claimed before.

III) Reinterpretation of published data on the Pu-O system suggest, that above 650° C the α-phase is separated from the highly oxygen deficient γ-phase (PuO_{2-x}) by a narrow two-phase region $\alpha + \gamma$ in the range $1.69 \leq O/Pu \leq 1.72$.

The variation of the low oxygen side of the boundary of the α-phase field with temperature near O/Pu = 1.62 is not yet known with certainty. Also the details of the transformation process and their variation with oxygen content for samples in the region $1.70 < O/Pu < 1.995$ cannot be explained at present.

KEYWORDS

PLUTONIUM OXIDES
METALLOGRAPHY
X-RADIATION
DIFFRACTION
PHASE DIAGRAMS

C O N T E N T S

A METALLOGRAPHIC AND X-RAY INVESTIGATION OF PLUTONIUM OXIDES AT ROOM TEMPERATURE(+)

1. INTRODUCTION

The low temperature range up to about 1000° C of the Pu-O system between O/Pu = 1,5 and 2,00 has been investigated repeatedly in part or as a whole by dilatometry (1), (2), (3), x-ray analysis (5), (6), electrical resistivity (4) and with the EMF-method (11). Metallography obviously has not yet been used in a systematic way.

For this reason work was started in Karlsruhe at the beginning of 1966 on the Pu-O phase diagram with metallography and x-ray analysis with the aim to correlate the results of these two experimental tools. The starting point was the phase diagram by Gardner, Markin and Street (5) shown in fig. 1. It is based mainly on high temperature x-ray analysis of powdered oxides.

The main problem in the Pu-O system at present seems to be the question if a eutectoid exists at O/Pu = 1,71 as proposed by Chikalla et al. (6), if a continuous solid solution between α-Pu_2O_3 and PuO_2 exists as proposed by Gardner et al. (5) or if α-Pu_2O_3 and PuO_2 are separated somewhere by a narrow two-phase region above 650° C(++). This paper gives a contribution to clarify the situation from the point of view of experiment, a more general discussion and comparison of the Pu-O system with some rare earth oxide systems up to about 1200° C will be given elsewhere (14).

In order to present the results as clearly as possible, we shall use designations for the different phases in the Pu-O system as given in table I. This avoids the use of specified chemical compositions for phases which in fact may exist with a variable range of stoichiometries and furthermore the possibility of confusion between the two b c c phases of different oxygen contents is hoped to be at least minimized. The subscript 1 to α_1, see table I, for the C-type rare earth Pu_2O_3-structure stands for "low", since this phase only exists at low temperatures and with low oxygen content.

On the other hand for the α-phase the synonym C'-phase is proposed

(+) Manuscript received on June 19, 1967.

(++) This last point has been discussed extensively at an IAEA PANEL ON THE THERMODYNAMIC PROPERTIES OF THE Pu-O system at Vienna in October 1966.

in order to distinguish it from the C-type rare earth structure which has O/M = 1.5.

2. EXPERIMENTAL PROCEDURES

2.1. Preparation of starting material

The PuO_2 powder was prepared by precipitation of the oxalate and calcined at 900° C in oxygen. The powder was then granulated without binder, but for lubrification 0,4 % zinc stearate was used. It was compacted at 4 to / cm^2 and sintered at 1550°C under a nitrogen 8 % hydrogen gas mixture. The properties of the resulting pellets are given in table II.

2.2. Heat treatment and reduction to a given O/Pu-ratio

In order to prepare specimens of a given O/Pu-ratio, the pellets were reduced in a tube furnace at temperatures between 1400° C and 1600°C for times between about 2 hours to 24 hours. As reducing atmosphere hydrogen with different amounts of water (about 10 - 1000 ppm) or ultra pure hydrogen (purified by diffusion through a Pd-Ag alloy) were used. After some experience it was possible to produce with this method O/Pu-ratios not far away from the desired values. After a reducing treatment the pellet usually was quenched from 1400 - 1600°C to about 5° C. Several samples were cooled in the furnace to 600°, 500°, 400° or 300° C and annealed at one of these temperatures between one and 16 hours and then quenched to 5° C in the normal way.

2.3. Determination of O/Pu-ratio

After the heat treatment the oxygen content was determined by gravimetric analysis. Always two specimens of the quenched sample were oxidized to $PuO_{2,00}$, either in oxygen at 850° C or in a CO/CO_2 = 10 : 1 mixture at 850° C (Harwell). The two methods give essentially the same results. The precision of the method is about O/Pu $\pm$ 0,005.

2.4. Metallography

The samples are handled in glove boxes under dry nitrogen and mechanically polished following the usual classical methods. Chemical etching is used. In the range $2{,}00 \geq O/Pu \geq 1{,}70$ mixtures of HNO_3 + HF at temperatures up to 100°C (5-20 sec) are used. In the range below O/Pu = 1,70 H_2SO_4 conc. at the boiling point for 10-30 sec. works better. Occasionally H_3PO_4 at the boiling point (1 - 2 min.) was used for samples close to stoichiometric PuO_2.

2.5. X-ray analysis

Samples for both the Debye-Scherrer- and the diffractometer techniques were prepared by crushing the pellets in glove boxes kept under nitrogen. In a few cases solid specimens were investigated on the diffractometer to check for oxidation during crushing.

The x-ray diffraction patterns were obtained either with 114,6 mm diameter Debye-Scherrer cameras or with a Siemens diffractometer having a quartz crystal monochromator placed between specimen and counter. In all cases, CuK_α - radiation was used.

A description of the Debye-Scherrer cameras is given elsewhere (13). Their construction permits the handling and the mounting of the capillaries in a glove box whereas the x-ray source and the films are outside of the box. With this arrangement the possibility of contaminating the films is completely eliminated.

Calibrations of the cameras with gold, silver and tungsten powders yielded mean values of the lattice parameters within 2.10^{-4} Å of the best values reported in the literature. Ilford Industrial B x-ray film was used in the asymmetric Straumanis arrangement, line positions were measured to 0,05 mm and entered into a computer program executing the following operations:

1. Straumanis correction for obtaining the true film diameter.
2. Calculation of the Bragg angle of each line, with interplanar distance and in the case of complete cubic spectra

calculation of the lattice constant a.

3. For complete cubic spectra the function a = f ($\cos^2\theta$) is extrapolated to $\theta = 90^\circ$ for the high angle lines by a least squares method.

In cases where the cubic spectrum does not allow extrapolation to $\theta = 90^\circ$ and for non-cubic spectra an empirical correction curve $\Delta d = f(\theta)$ has been used to obtain the true d-values and lattice parameters. This proved necessary especially for determination of the lattice parameters of the α-phase which never gave reflections at high angles.

For work with the goniometer the specimens are loaded into a special container with a semi-cylindrical beryllium window. A procedure has been developed to load it with the specimen in a glove box without contaminating its outer surface. In the case of cubic spectra with sharp lines at high angles the same computer program was used including the extrapolation to $\theta = 90^\circ$, but with somewhat less precision than for films. With the α-phase the lattice parameter was calculated for each line observed and finally taken the mean of all values. The limit of error for the lattice parameters of well-crystallized cubic phases is about $\pm$ 0,0005 Å with the film technique and about $\pm$ 0,0008 Å with the diffractometer. Many of the α-phases observed were poorly crystallized and their parameters are not known better than to $\pm$ 0,01 Å.

The majority of the spectra was analysed for the half widths and ratios of intensities of the following pairs of lines :

γ-phase	111	200	220	311
α-phase	222	400	440	622

If the spectrum was recorded on film the line profiles were found by densitometry. The results are given in figures 4, 5, 6, 8 and 9 taking into account the instrumental half width b of the lines. This was determined as $b = 0{,}1^\circ$ on diffractometer recordings and as $b = 0{,}35^\circ$ on films for the angular position of the (622) line of the α and α_1-phases and of the (311) line of the γ-phase (PuO_2) respectively. The true half width ß is taken as ß = B - b,

where B is the observed half width. Thus for specimens which are very well crystallized the line broadening ß is taken as zero.

3. METALLOGRAPHY

3.1. General results

The photo micrographs M1 to M20 with a few exceptions show the metallographic structures of specimens quenched from 1400° - 1600° C to 5° C. The pictures are arranged in the order of increasing oxygen content of the specimens starting from O/Pu = 1,62 up to 1,995.

The as quenched structures can be divided into 4 groups, each group corresponding to a certain range of O/Pu. These groups and their subdivisions are shown in table III. The results for specimens with O/Pu $\leq$ 1,61 will be given in a later publication.

For the interpretation of the micrographs the transformation behaviour of plutonium oxides must be taken into account. By dilatometry (1), (2), (3) electrical resistivity (4) and by high temperature x-ray analysis (5) it has been established that the transformation at 650° C is rather quick and cannot be suppressed by normal quenching techniques. This implies rather high rates of the migration of oxygen when the high temperature phase is separated into two low temperature phases with very different oxygen content (see fig.1). Small variations in the rate of quenching may possibly give a very different geometry of the precipitates. An example is seen in the figures M16 a and b. These show a typical pearlite-like structure. The lamella spacing is very different in both specimens though the cooling rates were very similar. Probably the grain size plays also a role. On the other hand the integral O/Pu-ratio itself certainly influences the mode of precipitation too.

For a detailed interpretation the phase relations at 1500° C and the transformation behaviour at 650° C and 350° C should

be known as function of the O/Pu-ratio, but this is not yet the case. Information on these points can be gained by holding the specimens at temperatures below and above the phase boundaries before finally quenching to 5° C. There is a certain risk especially at lower O/Pu-ratios that the specimens are slightly reoxidized during such low temperature annealing, therefore the oxygen content has to be checked after each treatment.

3.2. Region O/Pu ≤ 1,62

The two phase structures fig. M1 and M2 appear straight forward from the point of view of metallography. If one accepts that the line for cubic $PuO_{1,61}$ may be shifted to about $PuO_{1,62}$ in fig.1 we have an α-matrix with some traces of hexagonal ß. The latter phase is precipitated with a well defined crystallographic relationship with respect to the matrix. This could be caused by a rapid shear transformation on (111) planes when crossing a phase boundary on quenching. Consequently the specimens would have been single phase at 1500° C according to this interpretation and the low oxygen boundary should be shifted to lower O/Pu-ratios with increasing temperature.

Yet another interpretation seems equally possible. The precipitation of the second phase may have taken place at rather low temperatures and it may consist of $\alpha_1 + \gamma$ instead of ß.

In this case the low oxygen phase boundary of the α-phase must have a different shape at high temperatures with respect to the first interpretation. In fig. 7, this interpretation is adopted and the low oxygen phase boundary of the α-phase is drawn as a dotted line. This problem will be discussed once more in section 4.5.

3.3. Region 1,627 ≤ O/Pu ≤ 1,69

A rather important result of this investigation is the existence of the single phase region shown in the fig. M3-8. In this range of oxygen content the α-phase can be quenched to room temperature with little difficulty. Only at O/Pu = 1,68 and 1,69, see

fig. M7 and 8a, one finds a fine substructure within each grain indicating the beginning precipitation of a second phase. In order to clarify this, specimens with O/Pu = 1,65, 1,676 and 1,69 have been furnace cooled from 1400 - 1600o C to 600°, 500°, 400° and 300° C, kept at least 1 hour at the low temperature and then quenched in the usual way. The results are shown in the fig. M5 a -c for O/Pu = 1,65 and 8 b and c for O/Pu = 1,69. For O/Pu = 1,65 the high temperature single phase region of α terminates between 400° and 300° C, for O/Pu = 1,69 this phase boundary certainly lies not far above 600° C, perhaps at 650° C. The resulting phase boundary which limits the domain of existence of the α-phase at low temperatures at the oxygen rich side is shown in fig. 7 to a first approximation.

3.4. Region $1{,}70 \leq O/Pu \leq 1{,}98$

Here the transformation occuring at about 650° C cannot be suppressed. Therefore the figures M9 to M20 show invariably two phase structures, but systematic changes in morphology as function of oxygen content occur. Infact one may subdivide this range in regions whose limits are approximately given in table III. Clearly more work is necessary in order to find the reasons for the striking changes with O/Pu-ratio under the same heat treatment in these specimens.

Since we may assume that all samples are single phase at 1500° C the amount of oxygen and its rate of migration certainly must influence deeply the morphology of the different two phase structures. But also ordering effects in the oxygen vacancy distribution may give some contribution.

Lineal analysis has been tried in this region in order to check the phase boundaries. Since this analysis had to be carried out on photographs the areas analysed were not sufficient to give precise values for the amounts of the two phases. On the other hand discrepancies occured between lineal analysis, x-ray analysis and calculated amounts around the composition $O/Pu \approx 1{,}78$ which cannot be explained by measuring errors and the causes are not known at present, see table V.

The results for the other regions 1,69 - 1,72 and 1,89 to 1,93 are also tabulated in table V in columns 8 to 10 together with an estimation of the relative amounts of the two phases by x-ray analysis and by calculations according to the phase diagram fig.7. With respect to the errors involved the agreement can be called satisfactory in these cases.

3.5. Region $1{,}98 \leqq O/Pu \leqq 2.00$

Following the phase diagram fig. 1 this region should be single phase γ, but metallography did not prove this.
Fig. M20 from a specimen with O/Pu = 1,995 $\pm$ 0,005 shows traces of a second phase and the sample of fig. M19 with O/Pu = 1,98 which was kept 1 hour at 700° C before quenching to 5° C has a very similar aspect as fig. 18. This points to a limit for the miscibility gap at $T \lesssim 500°C$ and $O/Pu \gtrsim 1{,}995$ instead of 1,98 as assumed before (5) (6). We shall refer to this point again in section 4.2 taking account of the x-ray results.

4. X-ray analysis

4.1. General results

As described in section 2,5 the x-ray data have been analysed in the following manner :

i) determination of lattice parameters and phases, see fig. 2 and 3 and table V.

ii) Correlation of the line profiles with the O/Pu-ratio of the samples in which structures have been produced by phase transformations at 650° to 350° C on quenching, see fig. 4, 5 and 6. A phase which has not changed or hardly changed its composition during quenching gives sharp and highly peaked lines indicating a well crystallized structure. On the contrary a phase precipitated at low temperatures from a matrix with different O/Pu-ratio gives broad lines with lower peaks. Fig. 6 gives an example of such a difference in line shape.

iii) Analysis of relative peak heights for the lines of different phases in the same specimen has been attempted in order to estimate the amounts of the phases present, see fig.8 and 9, and column 9, 12 and 13 in table V.

Before going into details, the following general results can be stated :

a) Specimens which are clearly single phase by metallography may show two or even three phases by x-ray analysis. This happens especially in the region $1{,}62 \leq O/Pu \leq 1{,}69$. Specimens at $1{,}69 < O/Pu \leq 1{,}70$ which appear two-phase by metallography may give as much as four different cubic phases by x-ray analysis.
The question arises if these "x-ray phases" have been produced on the surface of the samples during the preparation

of the powders from the solid specimens. To decide on this, solid samples were investigated on the diffractometer but no difference was noted against the powdered specimens. Though also in this case the production of a transformed surface layer cannot be excluded we believe that these phases exist also in the solid specimens and are distributed on a submicroscopic scale, therefore they cannot be revealed by metallography.

b) Lattice parameters and line profiles of two phase structures (by x-ray analysis) show characteristic differences in the regions $1{,}61 < O/Pu \leq 1{,}69$

$1{,}69 < O/Pu < 1{,}80$

$1{,}80 \leq O/Pu \leq 2{,}00$

These differences can be seen on the figures 3, 4, 5, 8 and 9.

c) Inspite of the low temperature the transformation at 350° C proceeds still rather fast and shows up both by metallography, see fig. M 5 b, c and by x-ray analysis, see table V No. 12. This specimen with O/Pu = 1,65 was furnace cooled from 1500° C to 300 ° C, kept for one hour at this temperature and then quenched. The lattice parameters correspond exactly to the low temperature equilibrium structure $\alpha_1 + \gamma$ as to be expected from fig. 7 or fig. 1.
If the high temperature phases in the region $1{,}62 \leq O/Pu \leq 1{,}72$ are quenched directly to 5° C, the low temperature transformations at 350° C to 600 ° C are suppressed partially and α-phases with $a < 11{,}04$ Å and γ-phases with $a > 5{,}396$ Å are produced as metastable transformation products, see fig. 3 and table γ. These metastable phases cannot be identified on the photomicrographs with the exception of figures M 7 and M 8 a.

d) Attempts have been made to deduce the relative amounts of phases present on photo micrographs showing two phase structures by comparing relative peak heights of x-ray lines. This analysis did not always give useful quantitative re-

sults, see section 3.4.4., but the general trend in the development of the quantity of α-phase present as a function of O/Pu-ratio comes out very clearly, see fig. 8 and 9 and section 4.3.1.

e) The limits of detectability for the α-phase and for the γ-phase are very different. Very faint traces of γ in α may still be found on films or goniometer recordings, even if they are not revealed by metallography.
The α-phase on the other hand cannot be established by x-ray analysis for oxides with O/Pu $\geq$ 1,94 though the second phase is clearly revealed by metallography, see fig. M 18. This is a consequence of the double cell edge of the α-structure with respect to the γ-structure.

4.2. The lattice parameter of stoichiometric PuO_2 and the limiting composition of PuO_{2-x} at 20° C

It has been shown that PuO_2 cannot incorporate excess oxygen in its lattice [7]. In table IV measured lattice parameters of PuO_2 oxidized in air or oxygen by various authors are collected, also the parameter of $PuO_{1,98}$ is given where available. The last value for PuO_2 in the table has been determined in the course of this work both with a Debye-Scherrer camera and with the goniometer. Each apparatus was checked for correct alignment as indicated in section 2.5. The lattice parameter compares well with the results of [9]. The results of table IV give the lowest values a = 5,395$_2$ Å for the purest specimens of $PuO_{2,00}$. We may conclude therefore that the commonly accepted lattice parameter for PuO_2 a = 5,396 Å is somewhat too high, and pertains to impure PuO_2. The necessity for this redetermination arose because the lattice parameter and O/Pu-ratio of the γ-phase in two phase α+γ specimens at T < 350° C as found here, did not agree with the values a = 5,405 Å and O/Pu = 1,98 given in the literature [5], see table IV.

From fig. M 19 and section 3.5 on metallography we know that an oxide with O/Pu $\approx$ 1,995 still may show traces of a second phase after quenching from high temperatures. Furthermore, the lattice parameters of the γ-phase in oxides 1,72 $\leq$ O/Pu $\lesssim$ 1,995

which invariably have two phase structures $\alpha + \gamma$ after quenching from 1500° C show little scatter around a mean value, a = 5,3969 Å instead of a = 5,405 Å, see fig. 3. And finally, the specimen No.12 of table 5 which was slowly cooled to 300° C gives also a lattice parameter of a = 5,396 $\pm$ 0,002 Å for the γ-phase in equilibrium with α_1.

Consequently the phase boundary of PuO_{2-x} against the two phase region $\alpha + \gamma$ at $T \lesssim 450°$ C cannot lie correctly at O/Pu = 1,98, but must be moved to about 1,995. Fig. 1 has been corrected accordingly in fig. 7.

From fig. 3 another interesting conclusion may be reached. If oxides with $O/Pu \lesssim 1{,}72$ are quenched from 1400° C, or from some temperature above the phase boundary α against $\alpha + \gamma$ in the range $1{,}62 < O/Pu \leq 1{,}72$, the lattice parameter of γ in the resulting two phase structures increases with decreasing O/Pu-ratio from $a \approx 5{,}397$ Å at O/Pu = 1,72 to a = 5,425 Å at O/Pu = 1.65. Obviously the low temperature equilibrium composition of the γ-phase ($O/Pu \approx 1{,}995$) cannot be produced any more for $O/Pu <$ 1,72 though the quenching conditions are kept the same. Therefore, a metastable oxygen deficient γ-phase with a higher lattice parameter results. This is reflected also by fig. 4 which shows the line broadening of these γ-structures. The γ-phase with the highest lattice parameter also has the broadest lines, that is the structure which is least well developed.

4.3. The α-phase in the single phase region $1{,}62 < O/Pu \leq 1{,}69$

The domain of existence of the α-phase has been established in section 3.3 on the basis of metallographic evidence. Because the partial low temperature transformations not detected by metallography are revealed now, the interpretation of the x-ray data is more involved.

4.3.1. Lattice parameters and line profiles of the α-phase

In fig. 2 the lattice parameters of the main α-phase of quenched specimens with $1{,}62 \leq O/Pu \leq 1{,}69$ are plotted against O/Pu ratio. From this the lattice parameter

varies linearly between 10,95 ± 0,02 Å at O/Pu = 1,69 and 11,00 ± 0,02 Å at O/Pu ≈ 1,62 and these values have been employed in table I. The broadening of the corresponding x-ray lines is small or practically zero as seen from the group of points in the range $1{,}62 \leq O/Pu \leq 1{,}69$ at the bottom of fig. 5. This proves that this phase must have existed already at high temperatures with the same composition. The points indicating broad line profiles in the same O/Pu - region in fig. 5 belong to the secondary phases which have been produced in small quantities by the low temperature transformation on crossing the phase boundary which closes the α-phase field against the abscissa of fig. 7. This transformation follows either of two schemes depending on the integral oxygen content of the sample and/or on the quenching rate.

$$\alpha\ (x) \longrightarrow \alpha\ (x'\ ) + \gamma\ (x''\ )$$

$$\alpha\ (x) \longrightarrow \alpha_1 (x'''\ ) + \gamma\ (x''''\ )$$

The behaviour of the appropriate γ-phases with respect to lattice parameters and line broadening is found in fig. 3 and 4. It fits exactly to this interpretation. Finally in fig. 8 the intensity ratio $I(440)_\alpha / I(220)_\gamma$ is plotted against oxygen content of the samples and a very steep rise is found for $O/Pu < 1{,}70$. This again is consistent with an extended α-phase at high temperatures and for $O/Pu \leq 1{,}69$.

4.3.2. The structure of the α-phase

As already stated by several authors [5] [6] [12] the diffraction pattern of α-$PuO_{1,61}$ is body centered cubic at 20° C, but the basic fcc reflections of the γ-phase still exist and constitute part of the bcc-pattern. Rather often the bcc extra lines are very weak or cannot be found

at all and in these cases the α-phase can only be identified by its lattice parameter. At higher temperatures the existence of the bcc extra lines has not yet been proved with certainty [5].

Another peculiarity of the α-phase is the weakness or absence of high angle reflections. The highest reflections observed in this work had a sum $\sum_i h_i^2 = 144$.

For these reasons all diffraction patterns containing the α-phase have been searched carefully for the existence of bcc extra lines. The phases for which they could be identified have been marked by the letter b in column 7 of table 5. They are only present in specimens with O/Pu $\leq$ 1,72. Very often only one to three bcc extra lines could be found. The most numerous set of 10 extra lines exists in specimen No. 24 of table 5 with O/Pu = 1,72 which according to column 9 of table 5 contains about 70 % of the α-phase. The next numerous set of 7 bcc extra lines was found in specimen No. 11 with O/Pu = 1,65 which had been cooled slowly to 400°C. Several times the (134)-line has been found as strongest bcc-line in the patterns.

4.4. <u>The low temperature two phase region $\alpha+\gamma_1$ at $1{,}70 \leq O/Pu < 2{,}00$</u>

The finer details of the metallographic results of section 3.4 with the figures M9 to M20 and table III are hardly reproduced by the x-ray analysis. Only the subdivision of this region into a part $1{,}80 \leq O/Pu \leq 2{,}00$ and a part $1{,}70 \leq O/Pu \leq 1{,}78$ is indicated. This corresponds to the difference between the structures shown in the figure M12 and in figure M13, at O/Pu $\sim$ 1,79. For O/Pu $\geq$ 1,80 the lattice parameters of the γ_1-phase show little scatter and the line broadening ß is very small, see fig. 3 and 4. This corresponds to the photo micrographs M13 to M20. We may conclude that in this region under the quenching conditions employed the γ-phase can be produced easily with an oxygen content close to the low temperature equilibrium value γ_1.

On the other hand for O/Pu < 1,79 the lattice parameters of the γ-phase in fig. 3 show somewhat more scatter and the line width has risen suddenly to higher values with respect to O/Pu ≥ 1,80, see fig. 4. This indicates in fact a change in the way by which this phase is produced during the transformation. This can also be observed as the difference in the distribution of the two phases in fig. M12 and fig. M13.

The results on the estimation of the relative amounts of the α- and γ-phases present, have already been described in section 3.4.

4.5 The low oxygen boundary of the α-phase and the region O/Pu < 1,62

In section 3.2 two possible interpretations for this region have been put forward, but a final decision must wait for more experimental results in the range 1,50 ≤ O/Pu ≤ 1,62. Careful inspection of the x-ray films of the specimens No. 2 and 3 of table V did not show any traces of the ß-phase. After this, the peak heights of the (622)- and (440)-lines of the two α-phases present were measured and are given in arbitrary units in columns 12 and 13 of table V. The figures show that a fair amount of the second α- (or α_1 -) phase must be present, together with a certain amount of the γ-phase. But about the same relations may also exist for other specimens up to O/Pu ≲ 1,72, as seen in table V.

Since it is very unlikely that the precipitates in fig. M1 and M2 are α in α or α_1 in α, they should consist of the γ-phase. Precipitation of one cubic phase in another cubic phase with a similar morphology as shown in fig. M1 and M2 can be found in fig. M18 to M20. Therefore the structures shown in fig. M1 and M2 might be interpreted as α with some traces of γ.
The following considerations may also hint at this interpretation:
In principle there exists a way to check the limiting composition of the α-phase near 350° C by making use of the intensity ratios of x-ray lines. There are several specimens in which the amount of α_1 produced in the last transformation at 350° C

is negligible. These specimens appear single phase by metallography and two-phase $\alpha + \gamma_1$ by x-ray analysis. From the course of the phase boundary between 640° C at O/Pu = 1,69 to 1,64 at about 400° C in fig. 7, we see that a specimen with O/Pu = 1,69 which is truly single phase above 650° C will transform a bigger part to the γ-phase between 650° C and 350° C on quenching than for example a specimen with O/Pu = 1,64, because the latter crosses this boundary at much lower temperatures. Now one can plot the relative intensities of the $(440)_\alpha$ and the $(220)_\gamma$-lines as amount of α-phase in %

$$\frac{I\ (440)_\alpha \times 100}{I\ (440)_\alpha + I(220)_\gamma}$$

against O/Pu-ratio and one can extrapolate this curve to 100 % α-phase in order to get the maximum oxygen content of the α-phase at 350° C. This has been done in fig. 9. Of course one cannot expect a high precision from this analysis, but it seems possible that the α single phase field at 350° C terminates at O/Pu$\approx$1,63 instead of 1,62. This interpretation is adopted tentatively in fig. 7.

5. DISCUSSION

The most important results of this investigation is the existence of an extended region of the α-phase at T$\gtrsim$ 650° C with 1,62$\lesssim$O/Pu$\leq$ 1,69. The boundary $\alpha/(\alpha + \gamma_1)$ below 650° C has been established mainly by metallography. The corresponding boundary at the low oxygen side as shown in fig. 7 is based on preliminary metallographic and x-ray results, but it has to be substantiated by further experimental work. The room temperature lattice parameters of the quenched α-phase are given in fig. 2.

In order to see if this result can be reconciled with the work of Gardner et al. [5], their corrected high temperature lattice parameters [15] for O/Pu = 1,618, 1,67 and 1,69 have been extrapolated to 20° C and these three points are shown as big squares in fig.2. They fit well into the parameter - composition relation of the α-phase as determined at 20° C in this work, Another interesting

observation can be made if the high temperature lattice parameters of [5] are plotted against O/Pu-ratio at 700° C and 900° C [14]. Both curves show a small but clear irregularity in the region $1{,}69 \leq O/Pu \leq 1{,}72$. In fact, together with other evidence this can be taken as indication for a small two-phase region at $T > 650°$ C separating the α-phase from the PuO_{2-x} phase [14]. Therefore this two-phase region has been indicated by a dotted line in fig. 7.

In a recent discussion Mulford has treated the relations between the three cubic structures PuO_2, $PuO_{1,50}$ and $PuO_{1,61}$ [12].

The α-phase has been assumed by Mulford still to exist only at a single composition $PuO_{1,61}$. Following him, it can be produced from the cubic $PuO_{1,50}$ structure (C-type rare earth structure) by inserting extra oxygen into the ordered oxygen vacancies. The unit cell of $PuO_{1,50}$ contains 32 Plutonium atoms, 48 oxygen atoms and 16 oxygen vacancies in an ordered arrangement which fits the body centered cubic symmetry. In order to maintain this symmetry, Mulford points out that any extra oxygen which is introduced into this structure, should have random distribution on the 16 vacant oxygen sites. For the α-phase, he assumes as the most probable composition 4 extra oxygen atomes giving $O/Pu = (48 + 4)/32 = 1{,}625$ This agrees very well with the lower limit of the α-region as found in this investigation.

Since the four extra oxygen ions are distributed statistically in the unit cell and there are still many lattice positions available in the oxygen sublattice it should be possible to place some more oxygen ions as long as there are still enough lattice positions vacant to give random distribution. If we take 6 instead of 4 we get

$$\frac{O}{Pu} = \frac{48 + 6}{32} = 1{,}6875 ;$$

again this value is about the same as found experimentally as the upper limit of the O/Pu-ratio for this phase.
The difference in the diffraction patterns of the two bcc structures $PuO_{1,50}$ and $PuO_{1,625}$ as calculated by Mulford [12] consists only in different ratios for the intensities of the two lines with $\sum_i h_i^2 =$ 190 and 192. Unfortunately it was not possible to check this,

since the highest value found in this investigation is only $\sum_i h_i^2$ = 144. On the other hand, the most intense line as calculated by Mulford should be (134) and this again agrees well with our results, see section 4.3.2.

The lattice parameters of the α-phase in the region 1,625 ≤ O/Pu ≤ 1,685 of fig. 2 can be extrapolated to lower O/Pu-ratios in order to find the room temperature equilibrium value of the α_1-phase. From a least square analysis of the corresponding points in fig. 2 a straight line can be drawn which gives a = 11,076 Å at O/Pu = 1,515, the oxygen content of the α_1-phase assumed by Gardner et al. [5]. This lattice parameter is somewhat higher than the highest values measured by these authors (a = 11,058 Å) and as found in this work (a = 11,06 ± 0,02 Å).
This result is reasonable since the measured values should be expected to lie below the true equilibrium lattice parameter. The transformation at 350° C by which α_1 is produced certainly will always lead to a phase slightly rich in oxygen.

The shift of the limit of the low temperature single phase region PuO_{2-x} from O/Pu = 1,98 to about O/Pu = 1,995 in fig. 7 is based both on metallographic evidence (see fig. M 19 and 20) and on lattice parameters, see fig. 3. The influence of a higher content of impurities in the earlier work [5] [6] seems the only possible explanation. The change in lattice parameter with substoichiometry da/dx for the region was about 0,45 Å = (5,405 Å - 5,396 Å)/0,02 according to [5]. The corresponding result in this work is da/dx= 0,30 Å = (5,3967 Å - 5,3952 Å)/ 0,005.

The two values can be considered roughly as equal if one thinks of the errors involved in the values of the lattice parameters and especially in the values of x.

In the phase diagram all phase boundaries which seem sufficiently well established at present have been drawn with full lines, the rest is indicated by dotted lines. A small two-phase field $\gamma_1+\gamma_2$ has been introduced in order to fit the existence of the two-phase region α + γ with the rest of the known phases to a reasonable pattern, which is in agreement with the phase rule [14]. Possibly this has to be modified when more detailed experimental data

become available.The results presented in this paper show that the Pu-O system is not yet completely established even at low temperatures.

Acknowledgements

We should like to thank Mr. E. Zamorani and Mr. K. Richter for preparing the starting material of this investigation and Mr. L. Angeletti and Mr. K. Buijs for the analysis of the impurity content.

REFERENCES

1.	N.H. Brett, L.E. Russel	Plutonium 1960, p. 397 Cleaver Hume Press
2.	T.D. Chikalla, J.M. Taylor	quoted in ref. 6.
3.	J.M. LeBlanc, H. Andriessen	EURAEC - 434 (1962)
4.	C.E. Mc Neilly	J. nucl. mat. 11, 53 (1964)
5.	E.R. Gardner, T.L. Markin, R.S. Street	J. Inorg. nucl. chem. 27 541 (1965)
6.	T.D. Chikalla, C.E. McNeilly, R.E. Skavdahl	HW 74802 (1962)
7.	E.E. Jackson, M.H. Rand	AERE - R 3636 (1963)
8.	W.H. Zachariasen	Acta cryst. 2, 388 (1949)
9.	C.R. Waterbury, R.M. Douglas, C.F. Metz	Analyt. Chem. 33, 1018 (1961)
10.	R.N.R. Mulford, F.H. Ellinger	J. phys. chem. 62, 1466 (1958)
11.	T.L. Markin, M.H. Rand	Thermodynamics Vol. I, p. 145. IAEA Vienna 1966
12.	R.N.R. Mulford	Paper submitted to panel on the thermodynamic properties of Plutonium Oxydes, IAEA Vienna, Oct. 1966.
13.	U. Benedict	Internal report No. 11 (1967) Institute of Transuranians, Karlsruhe
14.	H. Blank	EUR 3563 e
15.	T.L. Markin	Paper submitted to panel on the thermodynamic properties of Plutonium Oxydes, IAEA Vienna, Oct. 1966.

T A B L E I

Designation of phases and room temperature lattice parameters of Plutonium oxides as found in this investigation :

Phase	O/Pu	lattice parameter [Å]	structure
γ	2,00 2 - x	5,3952 ± 0,0005	fcc
γ_1	1,995 *)	5,3967 ± 0,0005	fcc
α	1,69 - 1,62	$10{,}95 \lesssim a \lesssim 11{,}01 \pm 0{,}02$	bcc C'-type
α_l	(1,51)	$11{,}03 \lesssim a \lesssim 11{,}07$	bcc C-type
ß	1,50		hexagonal A-type

*) γ_1 - phase in low temperature equilibrium with α or α_1.

T A B L E II

Properties of PuO_2 - specimens used as starting material in this investigation.

O / Pu	2,00
size	ø 5 mm, height 2 mm
density	about 95 % of theoretical
grain size	about 10 µ

Impurities :

C	25 ÷ 60 ppm
Al	$\lesssim$ 15
Mg	$\lesssim$ 20
Ni	$\lesssim$ 10
Mo	$\lesssim$ 10
Fe	$\lesssim$ 20
Si	$\lesssim$ 10
U	40

T A B L E III

Metallographic structures classified according to the O/Pu - ratios of the samples.

	O/Pu	No. of photo micrographs	phases present
1.	1,62	1,2	$\alpha + \beta$ or $\alpha + (\alpha_1 + \gamma)$
2.	1,627 - 1,69	3 - 8	single phase α in samples quenched directly to 5° C.
3.	1,70 - 1,995	9 - 20	$\alpha + \gamma$

According to the morphology of the quenched two-phase structures this region can be subdivided into

1,70 - 1,72	9,10	
1,76 - 1,78	11,12	
- - - - - - - - - - - -		Division as indicated by x-ray results, see section 4.4
1,80 -	13,14	
1,89 - 1,93	15-17	
1,93 - 1,995	18-20	

4.	1,995 - 2,00	

T A B L E IV

Lattice parameters of PuO_2 and $PuO_{1,98}$ from different authors.

	$PuO_{2,00}$	$PuO_{1,995} + \alpha$	Impurities	Reference
1.	5,3960 ± 0,0003	-	not stated	[10] [8]
2.	5,396 ± 0,001	5,405 ± 0,002 *)	550 ppm ***)	[5]
3.	5,395 ± 0,001	-	70 ppm	[9]
4.	5,3952 ± 0,0005	5,3967 ± 0,0005 **)	130 ppm	this work

*) In two phase specimen with an integral O/Pu-ratio of 1,717

**) average of many specimens containing γ in equilibrium with the α-phase

***) 100 ppm Mg 90 ppm Fe 150 ppm U

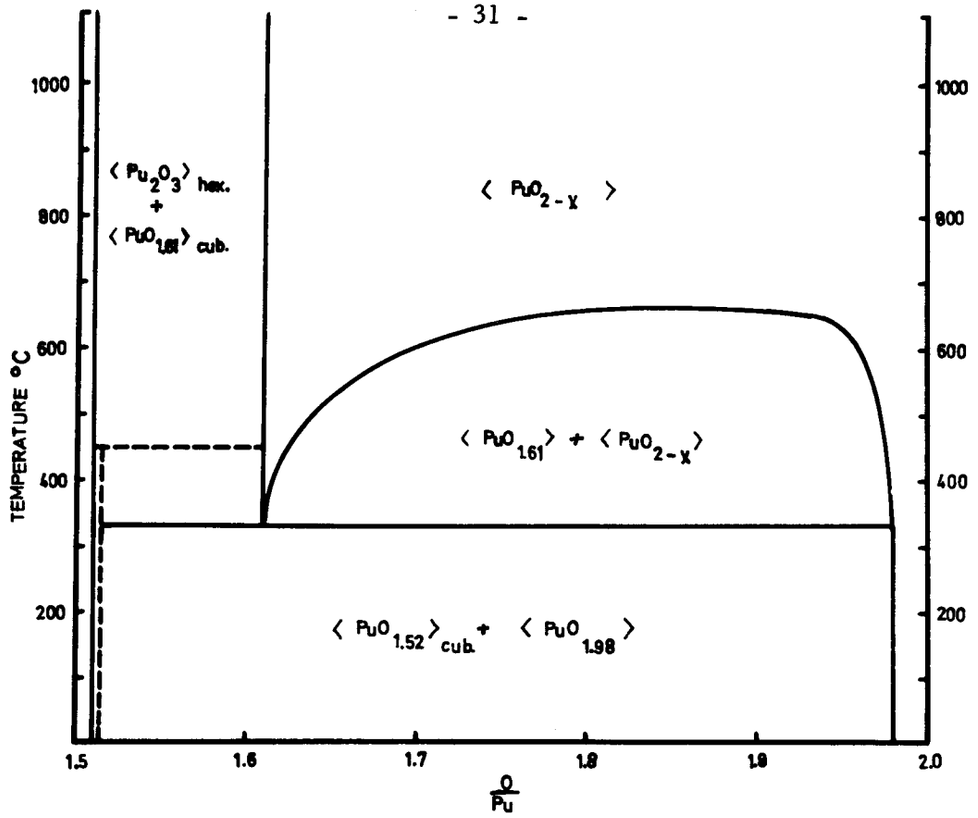

Fig. 1 - The Pu-O phase diagram [5].

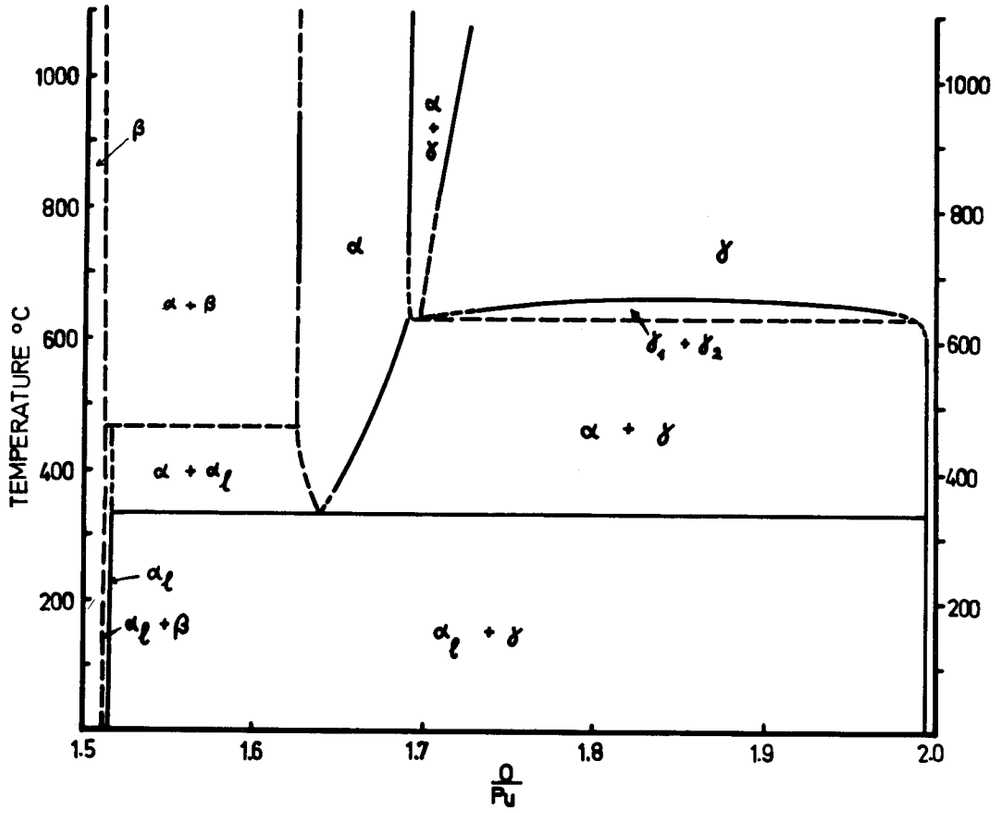

Fig. 7 - The Pu-O phase diagram modified on the basis of this investigation and of ref. [14].

Fig. 2 - Lattice parameters of the α-phase versus O/Pu-ratio at room temperature.

x : high temperature specimens

o : specimens held at 400 - 600°C

⊡ : values of [5] extrapolated to room temperature

The common field of errors for all points, except those of [5], is indicated by a narrow line. The abscissa is integral O/Pu-ratio, except for some specimens from the low temperature ($\alpha+\gamma$) field whose parameters are located at the limiting O/Pu of the α phase for the temperature concerned, taken from fig. 7. A least square straight line has been drawn for $1.62 < O/Pu < 1.69$, omitting point (11.02; 1.643).

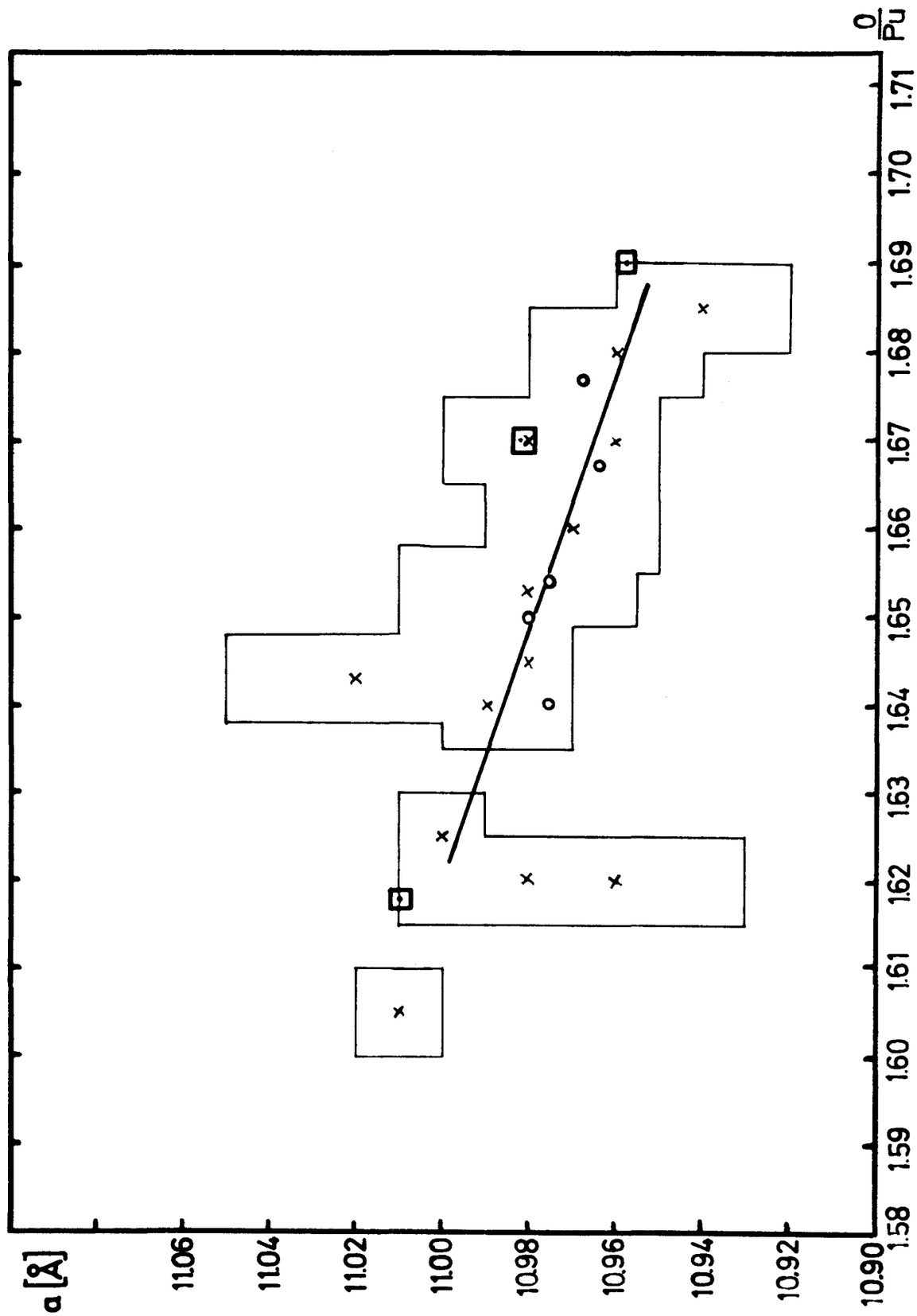
a [Å]
11.06
11.04
11.02
11.00
10.98
10.96
10.94
10.92
10.90
1.58
1.59
1.60
1.61
1.62
1.63
1.64
1.65
1.66
1.67
1.68
1.69
1.70
1.71
O/Pu

Fig. 3 - Lattice parameters of the δ-phase versus integral O/Pu-ratio as revealed by x-rays.

x : high temperature specimens

o : specimens held at 300 - 600°C

• : 2nd δ phase present in two specimens

The common field of errors is indicated as in fig. 2. The constancy of $\underline{a}$ in the range $1.80 \leq O/Pu < 2.00$ is indicated by a horizontal straight line at the average value $\underline{a} = 5.3967$.

Fig. 4 - Broadening of the (311)-line of the δ-phase versus integral O/Pu-ratio.

x : high-temperature specimens

o : specimens held at 300 - 600°C

Fig. 5 - Broadening of the (622)-line of the α-phase versus integral O/Pu-ratio of specimens containing two or more phases as revealed by x-rays.

x : high-temperature specimens

o : specimens held at 300 - 600°C

• : 2nd bcc phase (α or α_1) present in some specimens

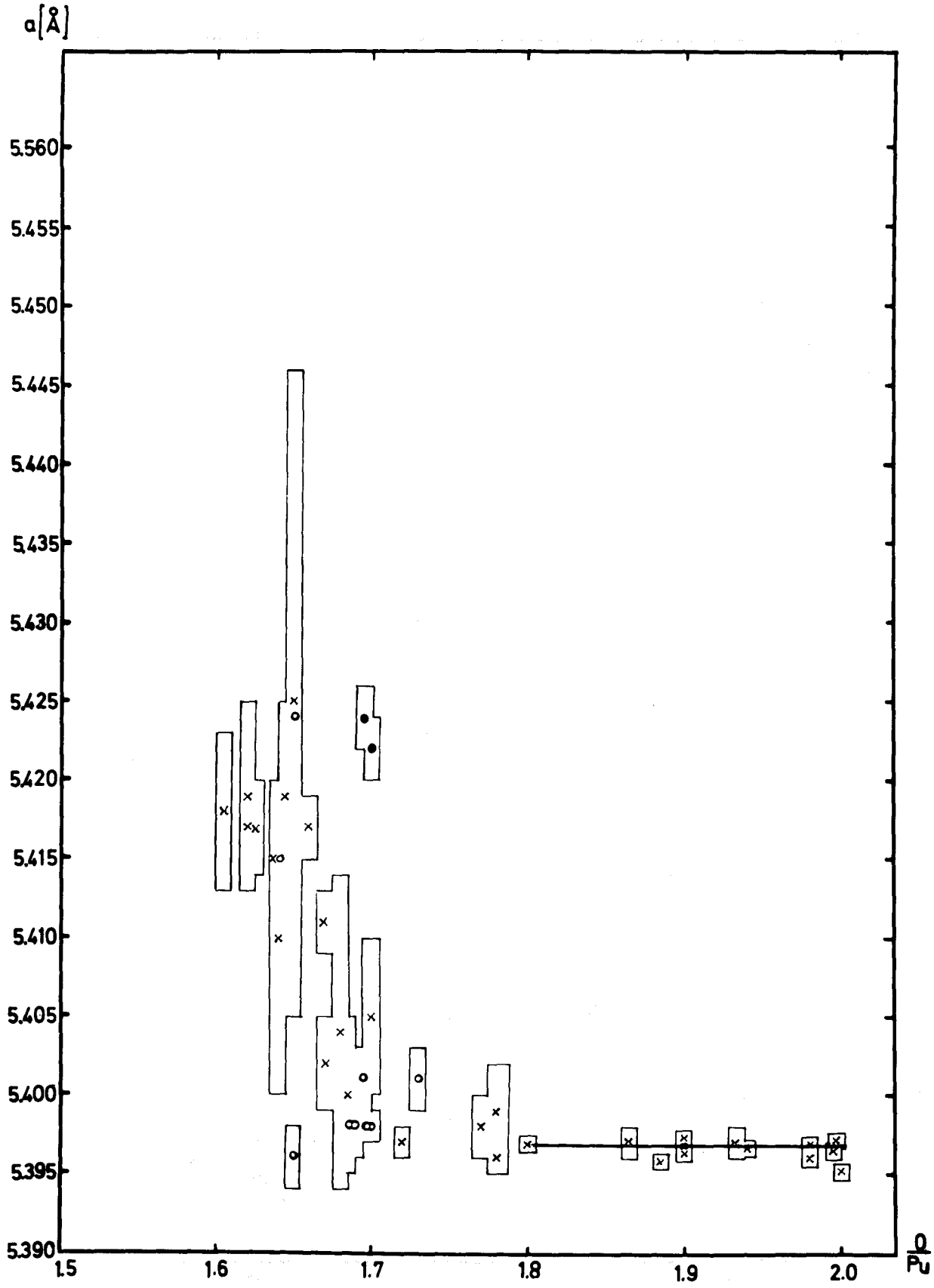
a[Å]
5.560
5.455
5.450
5.445
5.440
5.435
5.430
5.425
5.420
5.415
5.410
5.405
5.400
5.395
5.390
1.5
1.6
1.7
1.8
1.9
2.0
O/Pu

Fig. 3

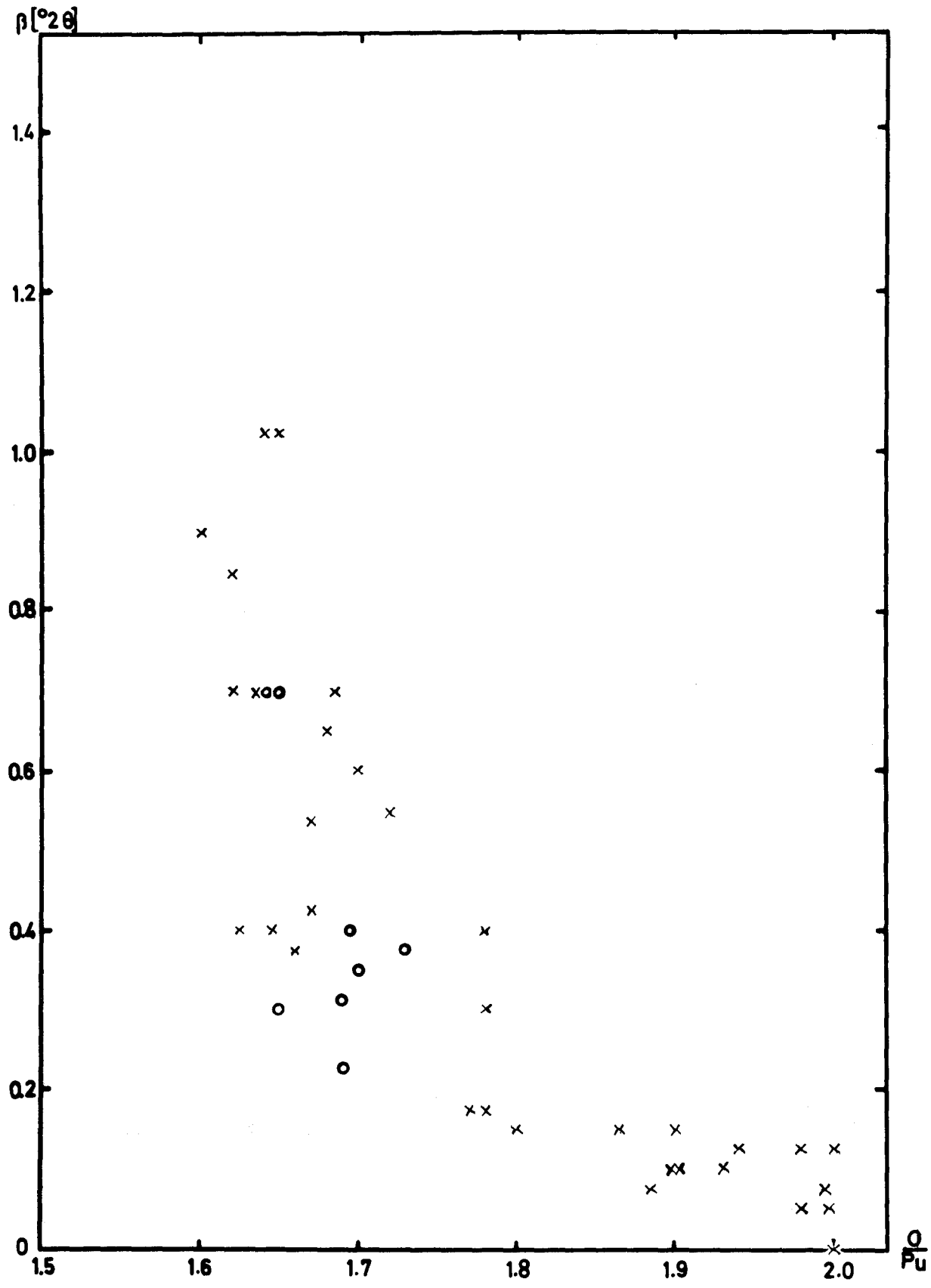

Fig. 4

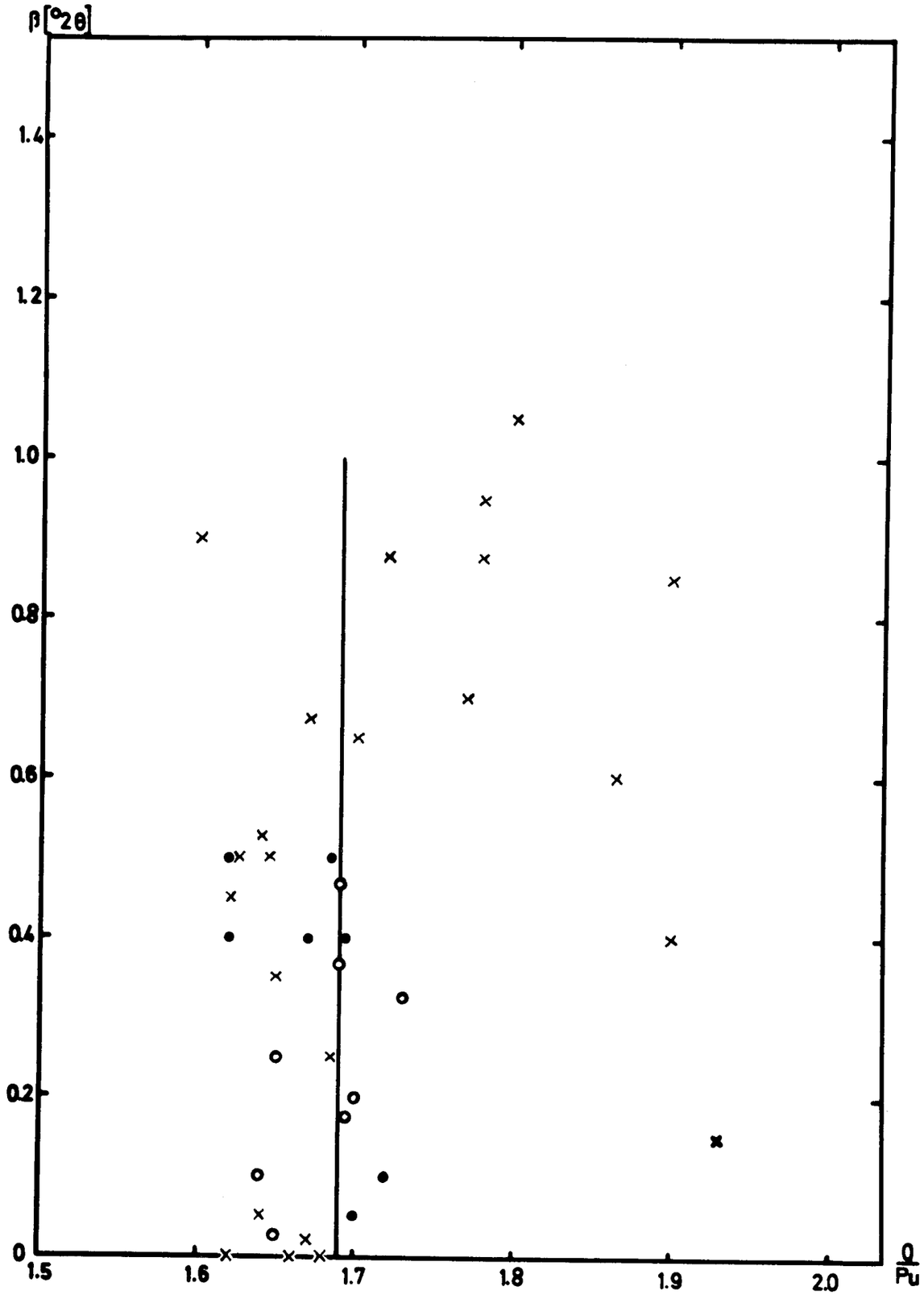

Fig. 5

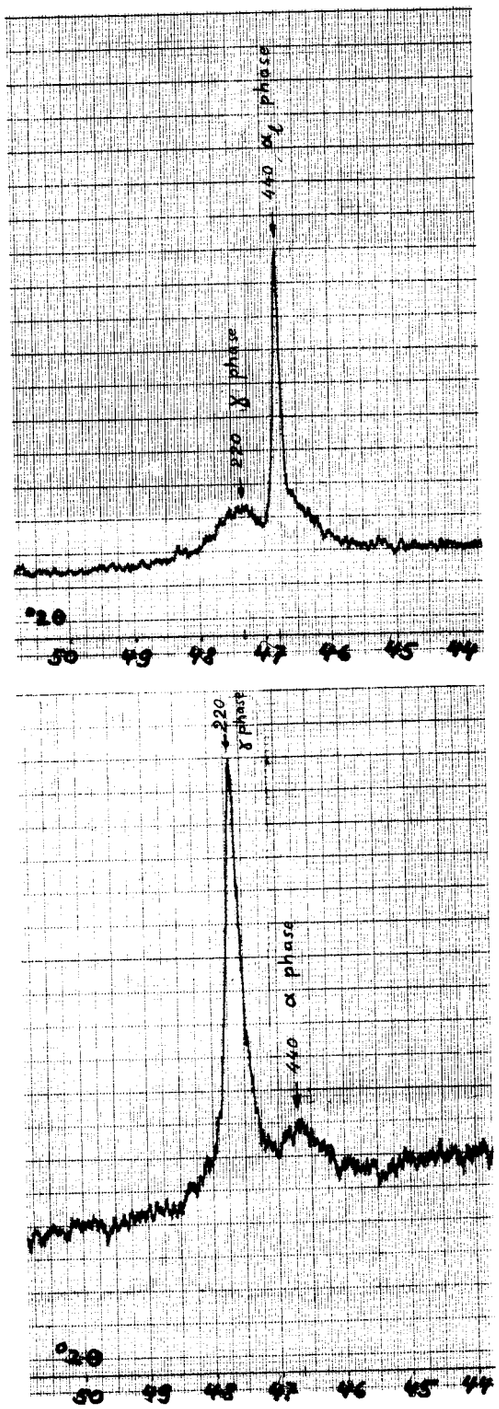

Fig. 6 - Typical x-ray line profiles as evaluated in the figures 4, 5, 8 and 9.

Above, $PuO_{1.65}$ held at 400°, same specimen as fig. M 5a.

Below, $PuO_{1.865}$ quenched from 1500°, same specimen as fig. M 14.

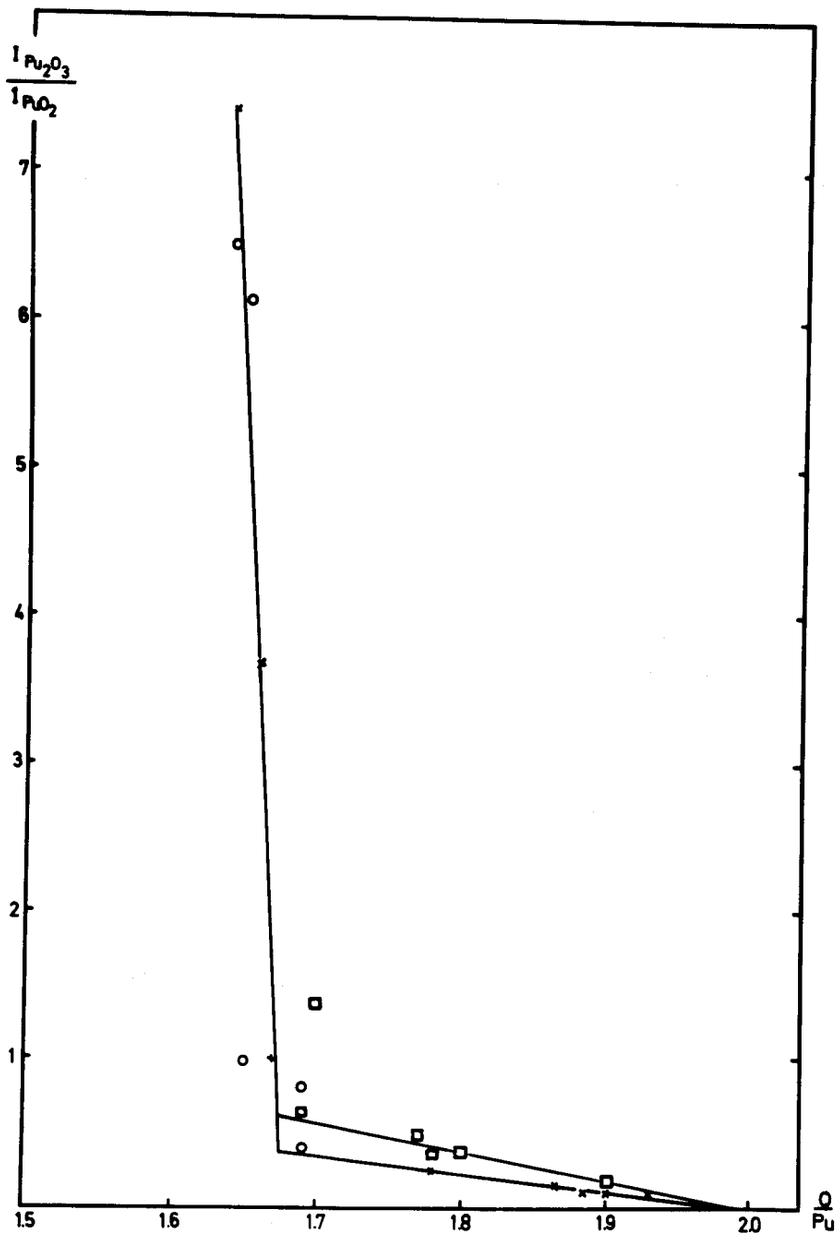

Fig. 8 - Intensity ratios I $(440)_\alpha$ / I $(220)_\gamma$ versus integral O/Pu-ratio of specimens containing two phases as revealed by x-rays.

For O/Pu <1.69, only diffractometer results are considered, as film techniques do not permit to see 3rd and 4th phases eventually present.

x : high-temperature specimens (diffractometer)

o : specimens held at 300 - 600°C (diffractometer)

□ : film results

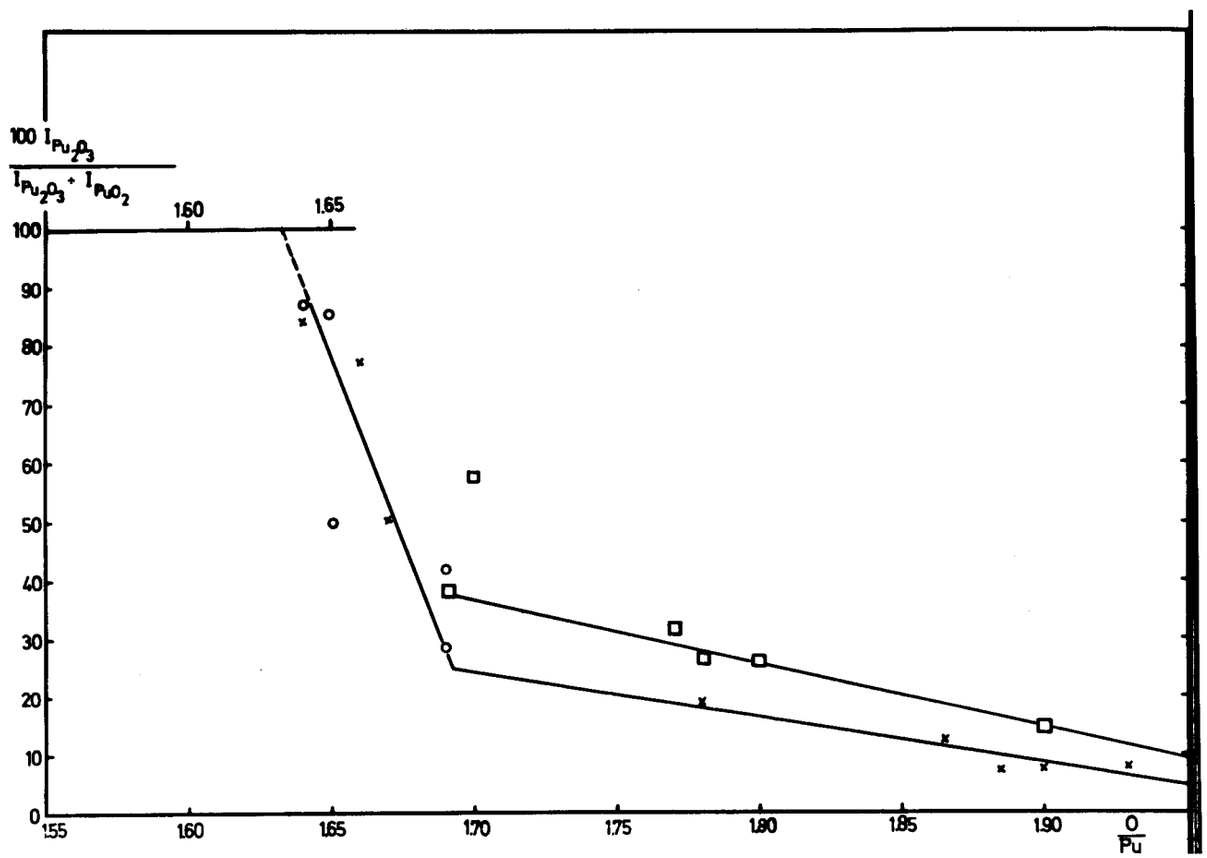

Fig. 9 - Same as fig. 8, but intensity ratios plotted as $I(440)_\alpha$ / $[I(440)_\alpha + I(220)_\gamma]$

Fig. M 1 O/Pu = 1,62 100 ×

Spec. 2, rapidly cooled, surface etched ;
traces of second phase are revealed as bright lines.

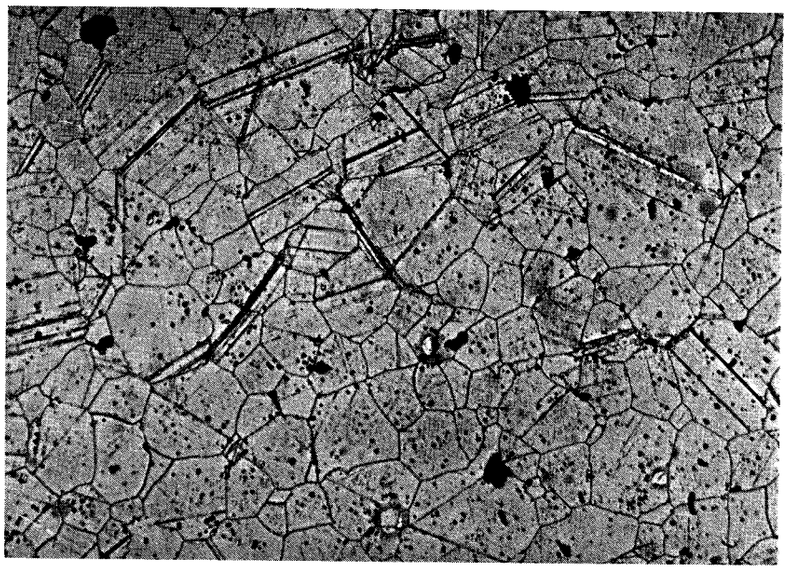

Fig. M 2 O/Pu = 1,62 200 ×

Spec. 3, treatment as specimen 2, surface etched.
Traces of second phase are revealed like grain boundaries.

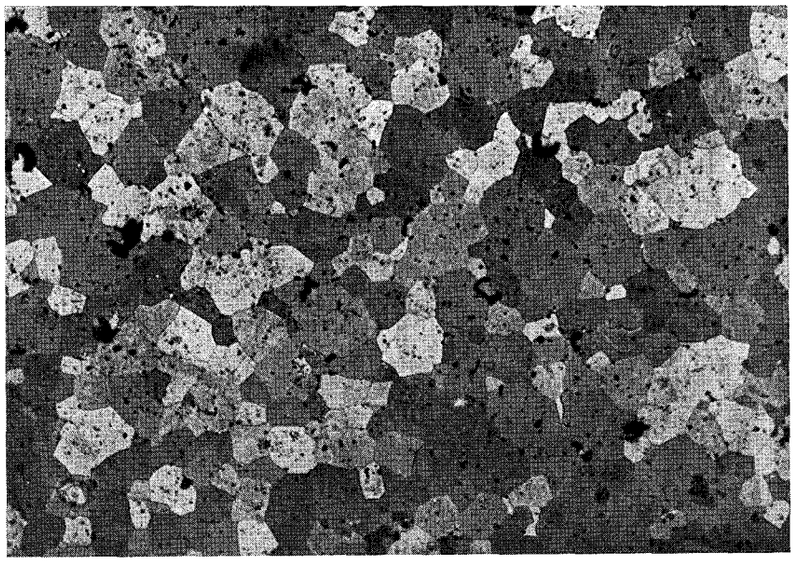

Fig. M 3 O/Pu = 1,627 200 ×
Spec. 5, quenched, α-single phase.

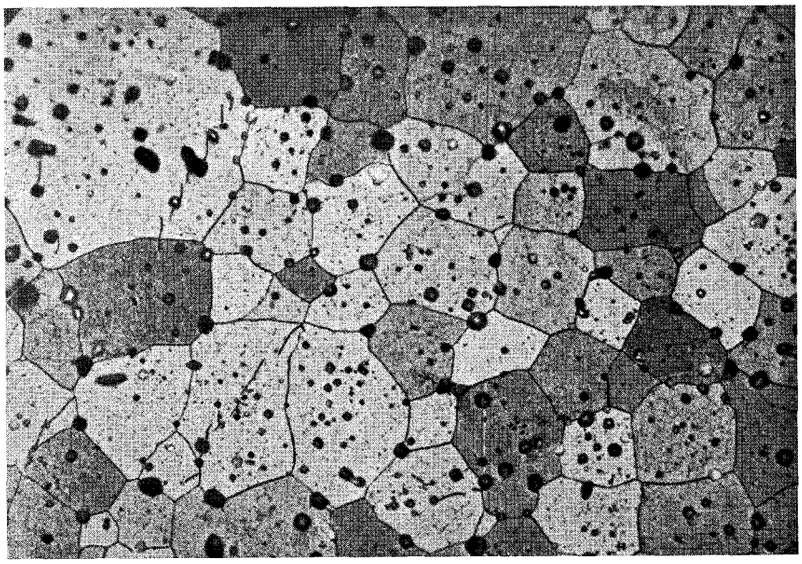

Fig. M 4 O/Pu = 1,643 500 ×
Spec. 8, quenched, α-single phase.

Fig. M 5a O/Pu = 1,65 200 ×
Spec. 11, quenched from 400 °C, α-single phase.

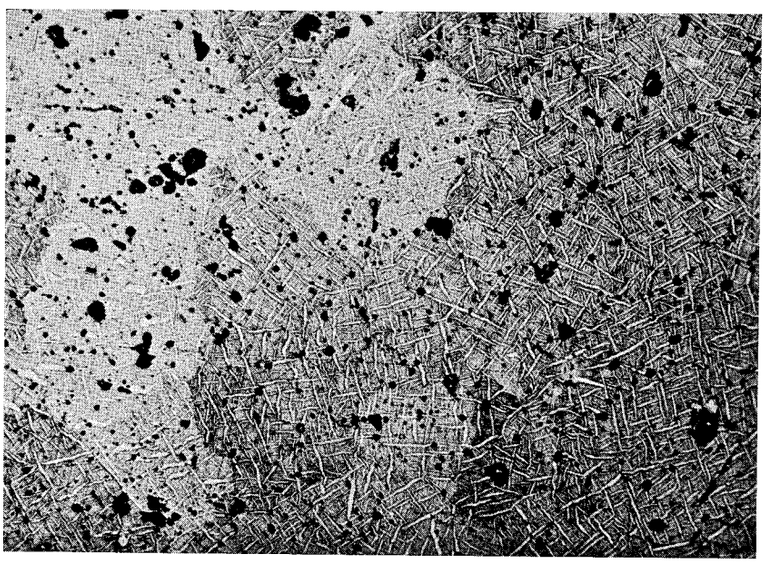

Fig. M 5b O/Pu = 1,65 200 ×
Spec. 12, quenched from 300 °C, two phase $\alpha_1 + \gamma$,
note difference to fig. M 5a.

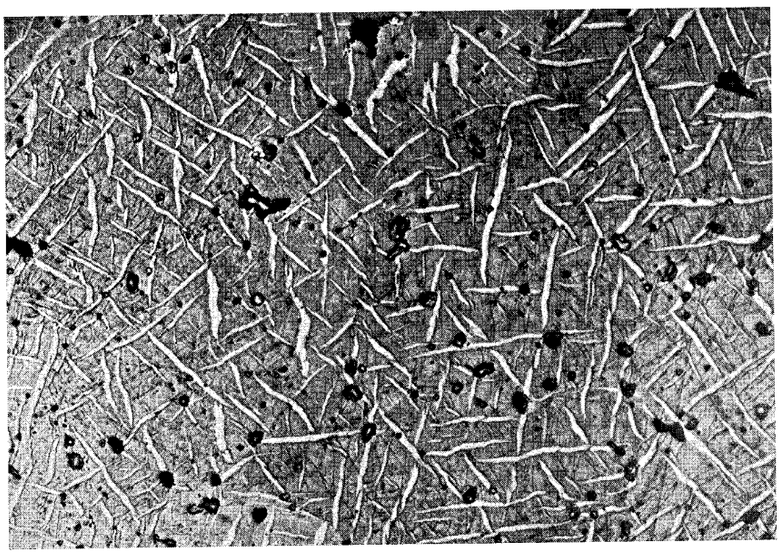

Fig. M 5c O/Pu = 1,65 500 ×

Same specimen and treatment as in fig. M 5b.

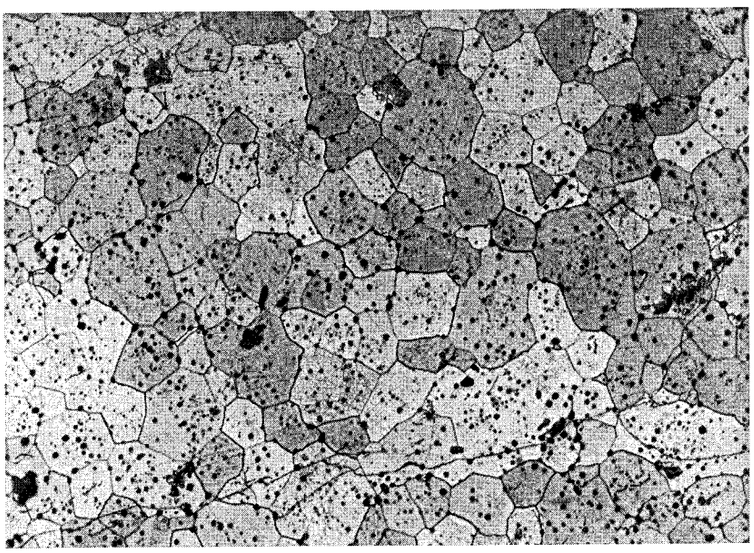

Fig. M 6a O/Pu = 1,66 500 ×

Spec. 13, quenched, α-single phase.

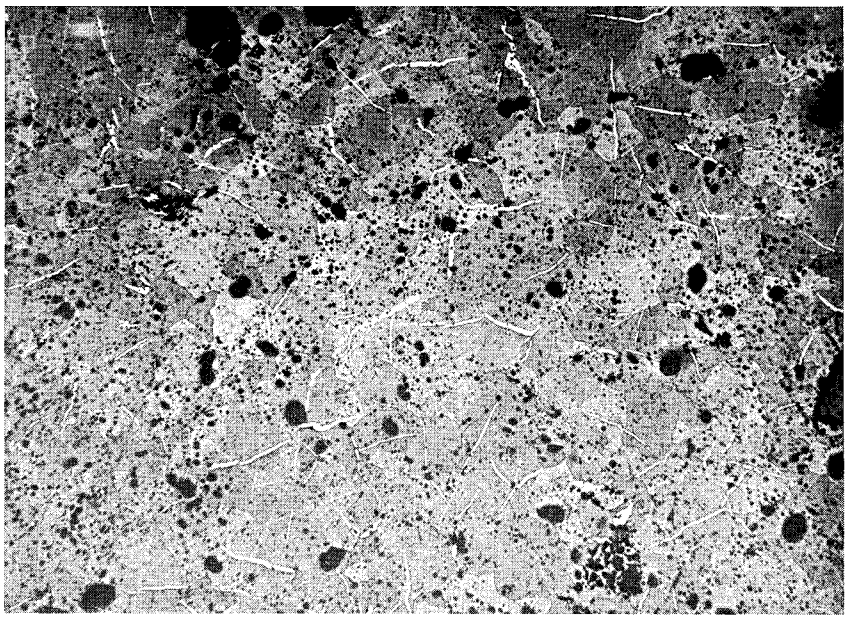

Fig. M 6b O/Pu = 1,676 100 ×

Spec. 15a, quenched from 500 °C.
At this temperature the specimen is slightly below the $\alpha/(\alpha + \gamma)$ phase boundary, see fig. 7, therefore some γ has been precipitated already.

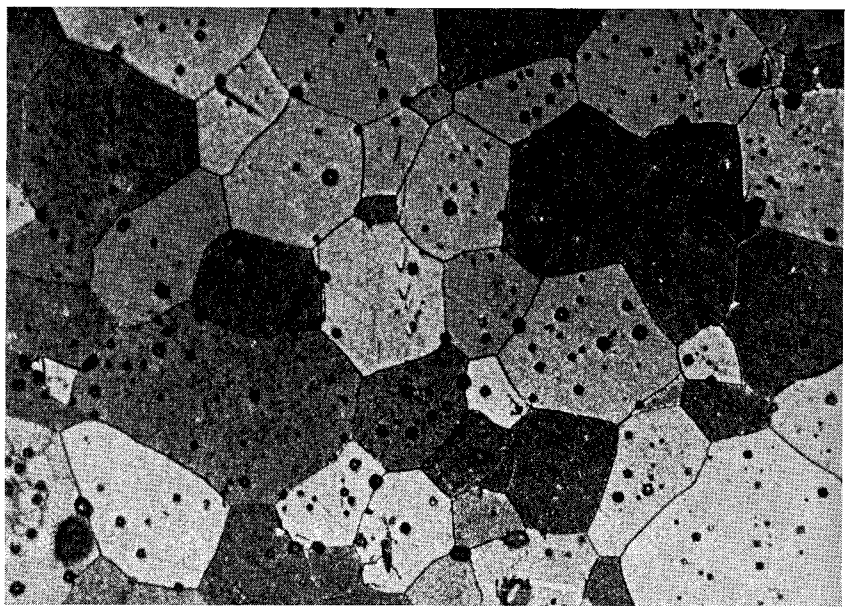

Fig. M 7 O/Pu = 1,68 500 ×

Spec. 16, quenched ; though the specimen is still α-single phase, a network of very fine precipitates can be seen within the grains. This has been produced during the last part of the quench.

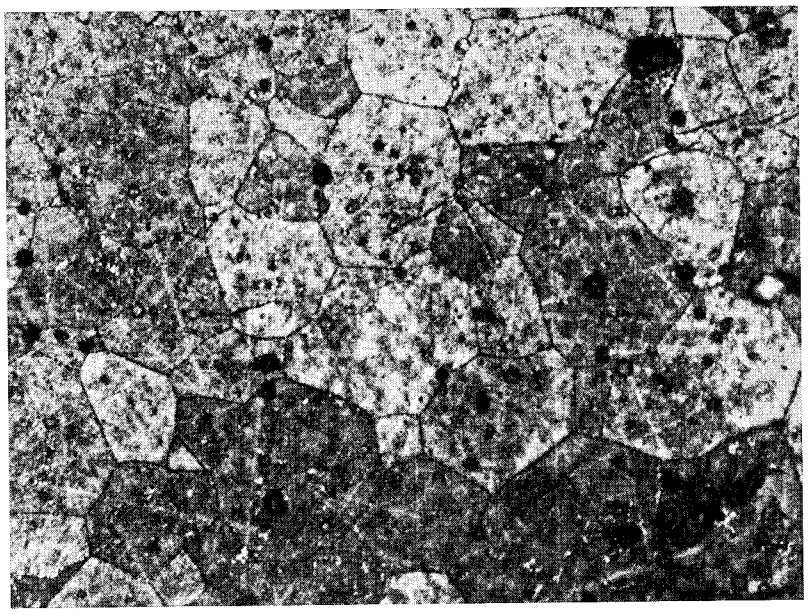

Fig. M 8a O/Pu = 1,694 500 ×

Spec. 18, quenched, same aspect as fig. M 7.

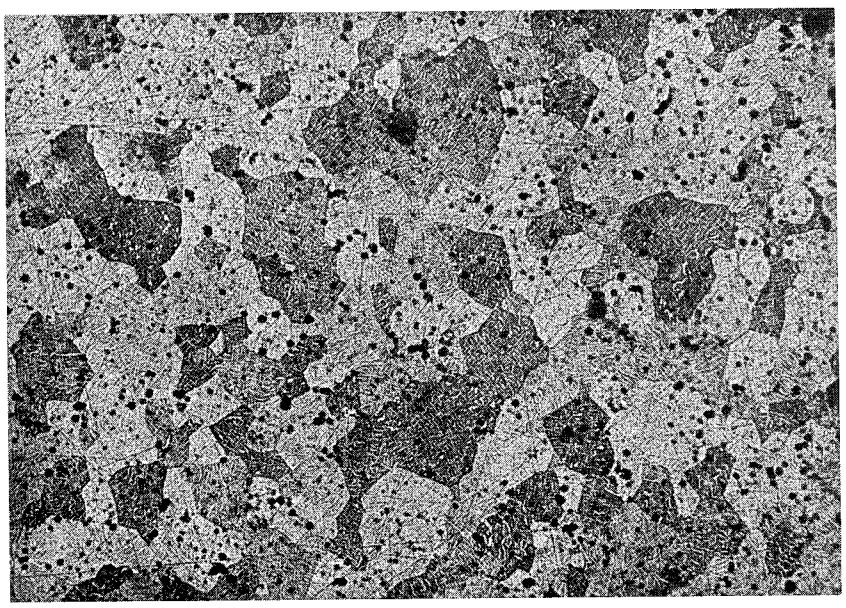

Fig. M 8b O/Pu = 1,69 200 ×

Spec. 19, quenched from 600 °C.
The α-single phase aspect of the structure is still preserved,
but precipitates within the grains have developed.
Compare with fig. M 7 and M 8a.
At 600 °C the sample obviously was slightly below the $\alpha/(\alpha + \gamma)$ phase boundary.

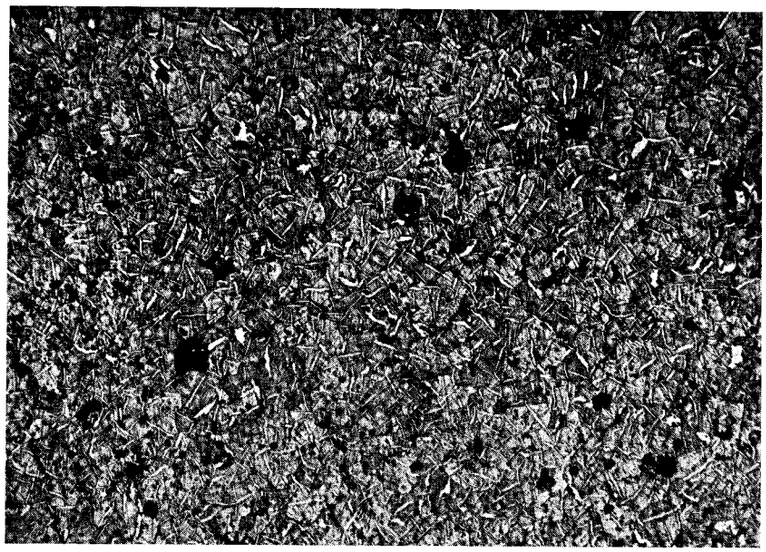

Fig. M 8c O/Pu = 1,69 200 ×
Spec. 20, quenched from 500 °C.
The structure now is clearly two phase.

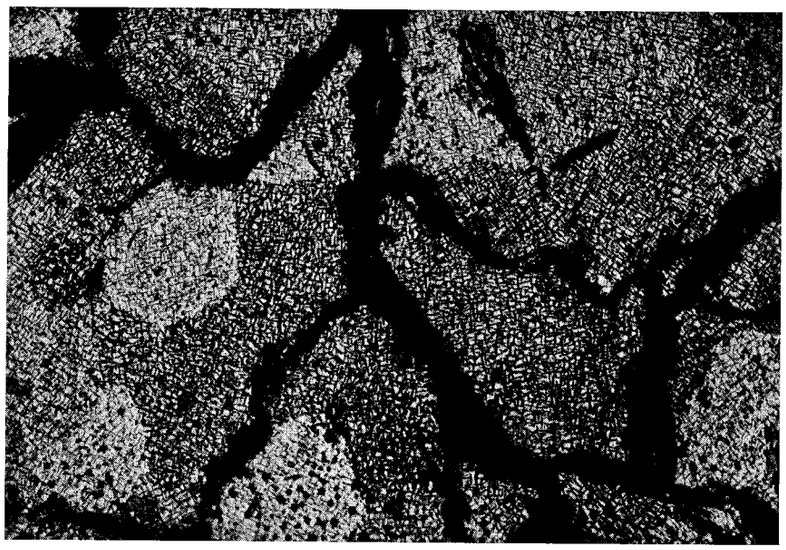

Fig. M 9a O/Pu = 1,70 200 ×
Spec. 23, quenched.
The as quenched structure is already two phase.

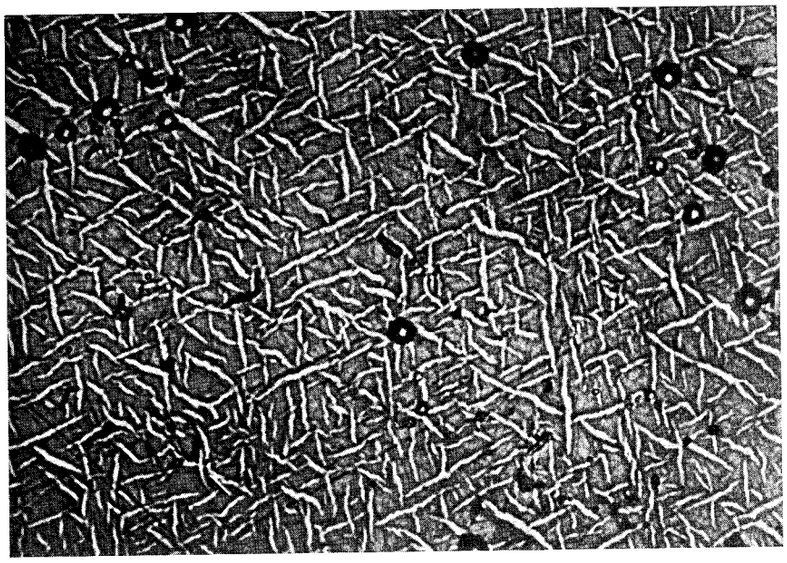

Fig. M 9b O/Pu = 170 1000 ×

Same specimen as fig. M 9a.

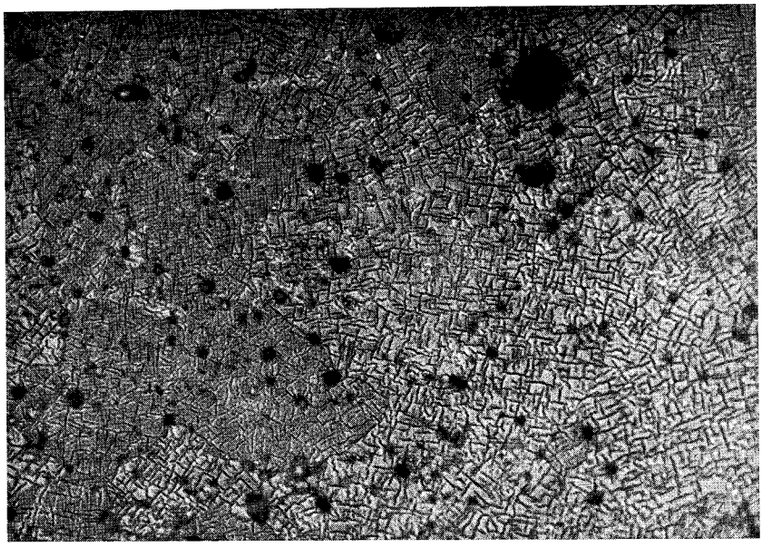

Fig. M 10a O/Pu = 1,72 500 ×

Spec. 24, quenched, two phases.

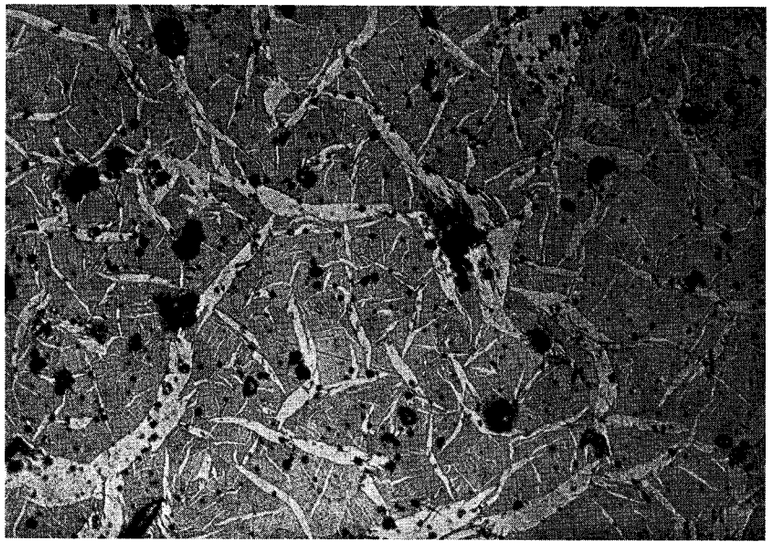

Fig. M 10b O/Pu = 1,72 200 ×

Spec. 26, cooled with about 300 °/h.
Different repartition of the two phases with respect to fig. M 10a.

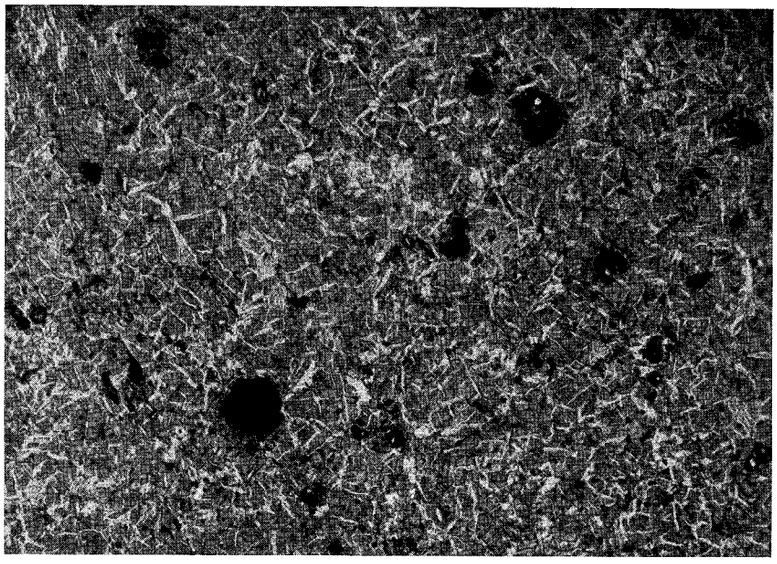

Fig. M 11a O/Pu = 1,76 200 ×

Spec. 27, quenched, two phases.

NOTICE TO THE READER

All Euratom reports are announced, as and when they are issued, in the monthly periodical **EURATOM INFORMATION,** edited by the Centre for Information and Documentation (CID). For subscription (1 year : US$ 15, £ 5.7) or free specimen copies please write to :

Handelsblatt GmbH
"Euratom Information"
Postfach 1102
D-4 Düsseldorf (Germany)

or

Office central de vente des publications
des Communautés européennes
2, Place de Metz
Luxembourg

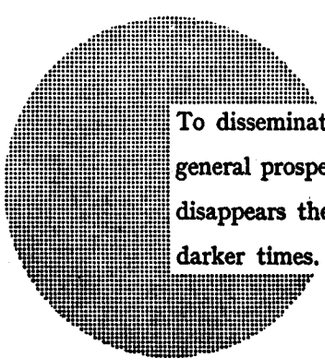

To disseminate knowledge is to disseminate prosperity — I mean general prosperity and not individual riches — and with prosperity disappears the greater part of the evil which is our heritage from darker times.

Alfred Nobel

SALES OFFICES

All Euratom reports are on sale at the offices listed below, at the prices given on the back of the front cover (when ordering, specify clearly the EUR number and the title of the report, which are shown on the front cover).

OFFICE CENTRAL DE VENTE DES PUBLICATIONS DES COMMUNAUTES EUROPEENNES
2, place de Metz, Luxembourg (Compte chèque postal N° 191-90)

BELGIQUE — BELGIË
MONITEUR BELGE
40-42, rue de Louvain - Bruxelles
BELGISCH STAATSBLAD
Leuvenseweg 40-42 - Brussel

DEUTSCHLAND
BUNDESANZEIGER
Postfach - Köln 1

FRANCE
SERVICE DE VENTE EN FRANCE DES PUBLICATIONS DES COMMUNAUTES EUROPEENNES
26, rue Desaix - Paris 15e

ITALIA
LIBRERIA DELLO STATO
Piazza G. Verdi, 10 - Roma

LUXEMBOURG
OFFICE CENTRAL DE VENTE DES PUBLICATIONS DES COMMUNAUTES EUROPEENNES
9, rue Goethe - Luxembourg

NEDERLAND
STAATSDRUKKERIJ
Christoffel Plantijnstraat - Den Haag

UNITED KINGDOM
H. M. STATIONERY OFFICE
P. O. Box 569 - London S.E.1

EURATOM — C.I.D.
51-53, rue Belliard
Bruxelles (Belgique)